ARTICLE

Synthesis of $Pb(OH)_2$/rGO Catalyst for Conversion of Sugar to Lactic Acid in Water†

Guan-hua Hou, Li-feng Yan*

Department of Chemical Physics, Collaborative Innovation Center of Chemistry for Energy Materials (iChEM), University of Science and Technology of China, Hefei 230026, China

(Dated: Received on February 26, 2015; Accepted on April 23, 2015)

Conversion of sugars from biomass to platform chemicals or fuels is an attracting topic for the utilization of biomass. Pb^{2+} ion is an efficient catalyst for the degradation of sugar to lactic acid, and it will be better to fix lead on a solid catalyst to reduce the risk of exposure of Pb^{2+} to environment. Here, a simple method has been developed to prepare a composite catalyst of $Pb(OH)_2$/rGO, where the nanoparticles of $Pb(OH)_2$ in size of 2−5 nm were prepared and fixed over the as-prepared reduced graphene oxide (rGO) nanosheets. The as-obtained catalyst showed an efficient catalytic activity to degrade glucose, fructose, and cellulose in aqueous solution, and the major product is lactic acid. The yield of lactic acid reached 58.7% when fructose was used as the feedstock (433 K and 2.5 MPa N_2), and the catalyst can be recycled with high activity. Cellulose can also be directly converted into lactic acid in aqueous solution over the catalyst without extra acid or alkali, and the maximum yield of lactic acid is 31.7%.

Key words: Graphene, Lead hydroxide, Nanoparticles, Composite, Catalyst, Lactic acid

I. INTRODUCTION

Lactic acid has attracted much attention for its abundant applications in pharmaceuticals, biodegradable plastics, food industry, and functional materials [1]. Currently, lactic acid is primarily produced by the fermentation of glucose, and this process has some disadvantages such as the formation of plenty of gypsum waste and cost due to multistep separation [2, 3]. So, new chemocatalytic processes for the production of lactic acid from cellulose are highly desirable [4]. Subcritical/supercritical water has been employed to convert glucose into lactic acid, but the process is also high-cost, especially at high temperature and pressure [5]. Recently, alkaline hydrothermal reaction has been utilized to prepare lactic acid from glucose, fructose, cellulose, and even directly from lignocelluloses [6, 7]. However, the employment of high concentration of alkali may corrode equipment and result in plenty of waste water.

Catalysts have attracted considerable attention in the efficient conversion of biomass to fuels or chemicals [8]. A few studies have been devoted to the direct production of lactic acid from polysaccharides or polyol by metal catalysts [4, 9, 10]. Dong *et al.* demonstrated that 62.8% of lactic acid was achieved after 30 min at 513 K under 2 MPa N_2 catalyzed by lanthanide triflates [11]. Jin *et al.* demonstrated that CuPd-graphene nanocatalysts could be used as catalyst for the conversion of glycerol to lactic acid with the addition of NaOH, a lactic acid yield of 45% was obtained after 6 h reaction at 413 K under 1.4 MPa N_2 [12]. However, the CuPd/rGO catalyst was limited only to the conversion of polyol such as glycerol, xylitol and sorbitol, and plenty of alkali was also needed in the study. Recently, Wang *et al.* reported that Pb^{2+} ion could catalyze the conversion of glucose, fructose or cellulose into lactic acid efficiently in water [13]. Yields of lactic acid of 68% or 62% were achieved for the conversion of ball-milled microcrystalline cellulose or microcrystalline cellulose at 463 K under 3 MPa N_2 for 4 or 15 h, respectively. Although promising, the direct use of $Pb(NO_3)_2$ solution as catalyst and the reutilization is difficult due to the toxicity and solubility of Pb^{2+} ions in water, which may hamper the practical application of this system. Is it possible to use nanoparticles of $Pb(OH)_2$ which was fixed on the surface of a solid carrier as an alternative catalyst?

Graphene has a large surface area and excellent mechanical properties, which is an ideal platform to anchor various functional groups or nanoparticles with accessible active sites for catalysts [14]. Recently, even graphene oxide (GO), the precursor of graphene, with a wide range of oxygen functional groups has been directly used as a catalyst for many reactions [15]. It is believed that functional modification of graphene or GO should promote new kinds of catalyst for green re-

†Dedicated to Professor Qing-shi Zhu on the occasion of his 70th birthday.

*Author to whom correspondence should be addressed. E-mail: lfyan@ustc.edu.cn

actions [16]. Supporting metal nanoparticles or ions on graphene nanosheets favor the large surface area and thermal stability of the catalyst for potential applications [17, 18].

Here, we try to prepare a composite of nanoparticle of $Pb(OH)_2$ and graphene, and use it as a solid catalyst for the lactic acid production from biomass based sugars.

II. EXPERIMENTS

A. Materials

Chemicals including formic acid, oxalic acid, glucose, 5-hydromethyl-furfural (HMF), and $Pb(NO_3)_2$ were all purchased from Sinopharm Chemical Reagent Co. Ltd. Microcrystalline cellulose (M_w=110 kg/mol) was purchased from Shanghai Hengxin Chemical Reagent Co. Ltd. D-fructose, analytical standard lactic acid, graphite powder (natural briquetting grade, about 100 mesh, 99.9995%, metals basis) were purchased from Aldrich. Analytical grade $NaNO_3$, $KMnO_4$, 98% H_2SO_4, 30% H_2O_2 aqueous solution and hydrochloric acid aqueous solution were purchased from Shanghai Chemical Reagents Company, and were used directly without further purification. Ultra-pure water (18 MΩ) was produced by a Millipore System (Millipore Q, USA).

B. Synthesis of $Pb(OH)_2$/rGO catalyst

GO was synthesized by a modified Hummer's method. Then 0.1−0.2 g GO powder was dispersed in 100 mL water under the assistance of ultrasound for 30 min. The GO nanosheets, containing of -COOH, -OH, and -CHO functional groups, can act as anchoring sites for the metal ions or nanoparticles. The GO dispersion was mixed with 30 mL aqueous solution of $Pb(NO_3)_2$ (0.036−0.1 mmol). The mixture was transferred to a round-bottomed flask and was purged with N_2 as a protecting gas under vigorous stirring, and then sodium borohydride ($NaBH_4$, 7.4−13.1 mmol) aqueous solution was gradually added to the mixture to reduce GO to reduced rGO. The mixture was stirred at 0 °C for 3 h, and then stood for another 2 h without stirring. The black solid products were isolated by filtration, washed with water, and it was dried in a freeze-dryer.

C. Characterization

Wide-angle X-ray diffraction (XRD) analyses were carried out on an X-ray diffractometer (D/MAX-1200, Rigaku Denki Co. Ltd., Japan). X-ray photoelectron spectroscopy (XPS) was recorded on an Escalab MK II photoelectron spectrometer (VG Scientific Ltd., United Kingdom). The thermal properties of the samples were recorded by a thermogravimeter (TGA, DTA-50, Shimazu), and all of the measurements were performed in N_2 over a temperature range of 30−800 °C with a ramp rate of 5 °C/min. Fourier transform infrared (FT-IR) spectra of the samples were recorded by a Bruker vector-2 spectrophotometer (Germany) using KBr-disk method. Transmission electron microscope (TEM) images were carried out on a Hitachi H-800 microscope at 200 kV. Inductive coupled plasma (ICP) was analysed by inductive coupled plasma emission spectrometer (Thermo Jarrell Ash Corporation, USA).

D. Catalysis activity test

Conversions of the biomass-based sugars were performed in a 50 mL pressure vessel (Parr Instrument, USA). Typically, 65 mg substrate, 25 mg $Pb(OH)_2$/rGO catalyst, and 15 mL water are added into the pressure vessel. After three cycles of purging the reactor with N_2, the pressure was set to 2.5 MPa with N_2. Then the reactor was heated using a 35 min ramp to a desired temperature, and the reaction was carried out under vigorous stirring. After reaction for a desired period of time, the reaction was quickly terminated by cooling the reactor to room temperature. The samples were analyzed by high-performance liquid chromatography (HPLC, LC-20AD, Shimadzu) on C-18-column equipped with an UV-Vis detector, and the retention time for lactic acid and HMF are 3.23 and 17.8 min, respectively. The conversion of fructose or glucose was determined on NH_2-column using a refractive index detector.

III. RESULTS AND DISCUSSION

Pb^{2+} ions were first adsorbed on the surface of GO nanosheets driven by the electrostatic interaction of the oxygen-containing groups of GO, and then it formed $Pb(OH)_2$ nanoparticles due to excess $NaBH_4$ added to GO solution while the GO nanosheets were reduced to rGO nanosheets. The structure of the as-formed product was measured by means of TEM, as shown in Fig.1. Clearly, some nanoparticles in size about 2−5 nm are formed on the surface of rGO nanosheets with an homogeneous dispersion, and the energy dispersive X-ray spectroscopy (EDX) analysis shows that the main chemical elements of the sample are C and Pb, while the signal of element Cu comes from the copper mesh supporting the sample for TEM measurement. The results revealed that $Pb(OH)_2$ in the complex was in the form of nanoparticles which anchored homogeneously onto the surface of rGO nanosheets.

The crystal phase structure of $Pb(OH)_2$/rGO composite was characterized by X-ray diffractometer. Figure 2 shows the typical XRD patterns of the com-

DOI:10.1063/1674-0068/28/cjcp1502026

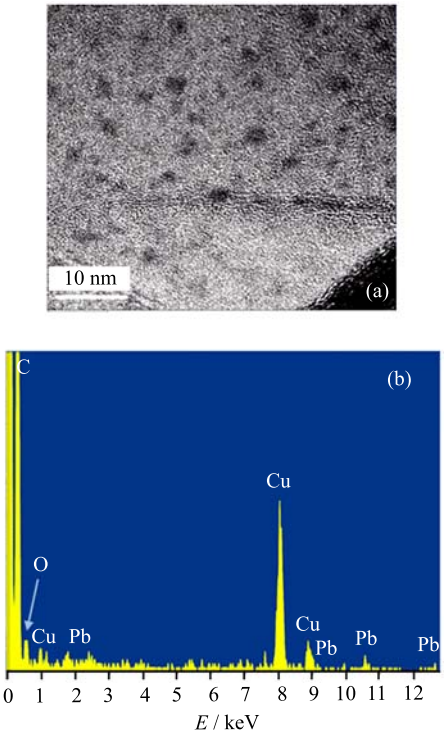

FIG. 1 (a) TEM and (b) EDX of $Pb(OH)_2$/rGO with 20wt% Pb loading.

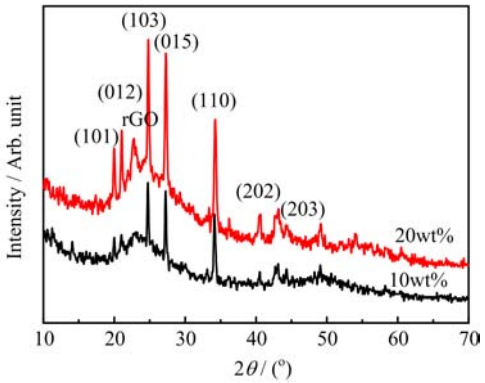

FIG. 2 XRD patterns of the $Pb(OH)_2$/rGO with 10wt% and 20wt% Pb loading.

posite prepared by loading 10wt% or 20wt% of Pb, respectively. There appears a wide peak at around 23.5°, revealing that the interlayer spacing of rGO nanosheets was about 0.37 nm after reduction, indicating the stacking of rGO nanosheets during reduction. In the curves, diffraction peaks can be indexed as $Pb(OH)_2$ (JCPDS card No.11-270). Clearly, the intensity of the diffraction peaks increased when the loading amount of Pb changed from 10wt% to 20wt%, indicating that the increase of Pb loading did not change its structure of crystalline but just made much deposition of nanoparticles in different sizes. The size of the $Pb(OH)_2$ nanoparticles calculated by means of XRD patterns were 2.3 and

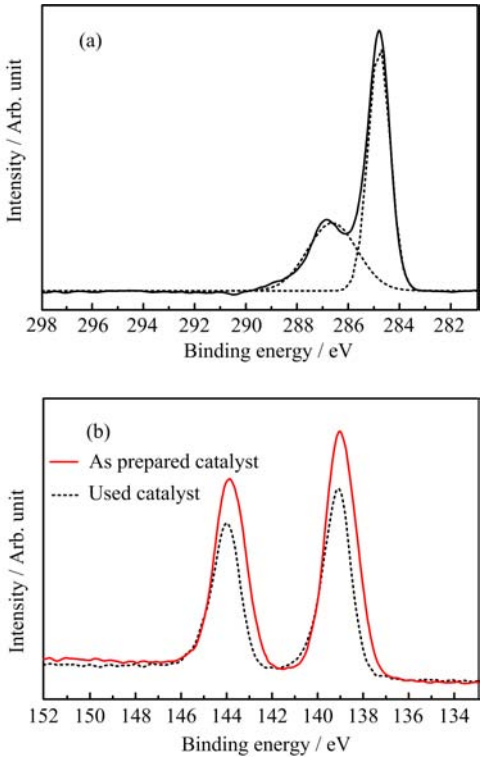

FIG. 3 XPS spectra of the $Pb(OH)_2$/rGO. (a) C1s pattern, (b) Pb4f pattern.

3.7 nm for 10wt% and 20wt% Pb loading catalysts, respectively, and the result was consistent with the TEM result.

Figure 3 shows both the C1s and Pb4f XPS patterns of the dried $Pb(OH)_2$/rGO powder. For Pb4f pattern, two main peaks locate at 139 and 144 eV, corresponding to the Pb $4f_{7/2}$ and $4f_{5/2}$ of $Pb(OH)_2$. For C1s pattern, the highest peak locates at 284.6 eV, corresponding to the C=C/C−C species. In addition, a weak peak at 287 eV appears, which is attributed to the residual oxygen-containing species of rGO, indicating the reduction of GO during the formation of the $Pb(OH)_2$/rGO nanocomposites. The amount of $Pb(OH)_2$ in the sample surface can also be calculated by means of the Pb4f XPS patterns, and there are 0.6mol% and 1.33mol% Pb for 10wt% and 20wt% Pb loading samples, coresponding to 8.9wt% and 17.8wt% of loading Pb. Additionally, the loading of Pb analysed by ICP and TGA (Fig.4) was 10wt% and 20wt%, respectively. So, the result of XPS was consistent with ICP and TGA.

The thermal stability of $Pb(OH)_2$/rGO podwer has been studied by TGA measurements in air. Figure 4 shows the TG curves of the samples with 10wt% or 20wt% lead loading. The rGO nanosheets will be completely decomposed when the samples were heated in air, and the residue should be PbO_2. Clearly for the 10wt% lead loading sample, the residual weight is about 10% while it is about 20% for the 20wt% Pb loading sample, indicating the added lead was nearly completely

DOI:10.1063/1674-0068/28/cjcp1502026

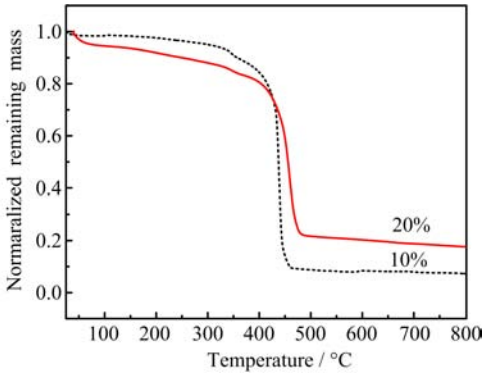

FIG. 4 TG curves of $Pb(OH)_2$/rGO.

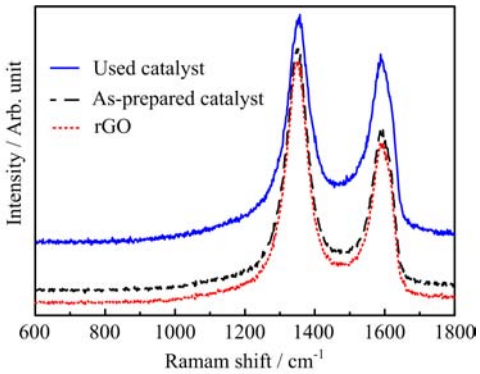

FIG. 5 Raman spectra of rGO, the used catalyst, and the as-prepared $Pb(OH)_2$/rGO.

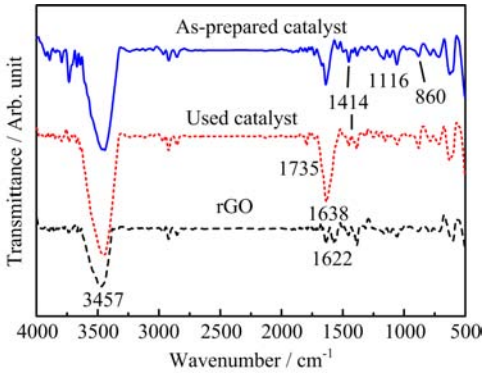

FIG. 6 FT-IR spectra of the as-prepared rGO powder, $Pb(OH)_2$/rGO, and the used catalyst.

TABLE I Catalytic performance of the $Pb(OH)_2$/rGO for the conversion C of fructose, glucose, and cellulose. Reaction condition: substrate of 65 mg, $Pb(OH)_2$/rGO (10%wt) of 25 mg, H_2O of 15 mL, N_2 of 2.5 MPa. LA denotes lactic acid.

Entry	Substrate	T/K	Time/h	C/%	Selectivity/%	
					LA	HMF
1[a]	Fructose	433	2	>99	18.0	12.7
2	Fructose	433	2	>99	48.9	1.9
3	Glucose	443	2	>99	39.5	1.3
4	Cellulose	463	10		27.6	0.01
5[b]	Cellulose	463	4		31.7	3.6

[a] Catalyst is rGO without addition of Pb.
[b] With addition of extra lactic acid to increase reaction.

reserved in the products.

Figure 5 shows the typical Raman spectra of rGO, the as-prepared $Pb(OH)_2$/rGO catalyst, and the used catalyst. All the spectra indicate the existence of the D and G bands of rGO nanosheets. For rGO powder, the G band is located at 1591 cm^{-1}, while for the $Pb(OH)_2$/rGO composite the peaks nearly locate at the same wavenumber. However, D band shifts from 1346 cm^{-1} to 1348 cm^{-1} after the formation of the complex catalyst. The intensity ratio of the D to G band (I_D/I_G) varies from 1.23 to 1.45, indicating the $Pb(OH)_2$ hybrids may affect the conjugated structures of the rGO [19].

Figure 6 shows the FT-IR spectra of the as-prepared and the used catalyst. For rGO, the characteristic peaks appear for C=O (1735 cm^{-1}), aromatic C=C (1622 cm^{-1}), carboxy C−O (1414 cm^{-1}), epoxy C−O (1228 cm^{-1}), and C−O (1116 cm^{-1}) [20], indicating the reduction is partial. We guess that the reduction of GO may be inhibited at the presence of $Pb(OH)_2$. For the as-prepared catalyst, the peak appearing at 860 cm^{-1} is the characteristic signal of symmetric stretching vibration modes of Pb−O bonds [21], and it reveals the formation of a composite of $Pb(OH)_2$ with rGO nanosheets in the as-prepared catalyst.

The above studies reveal the successful preparation of $Pb(OH)_2$/rGO composite, and it has been used as catalyst for the degradation of cellulose or its monosaccharide such as glucose or fructose to lactic acid in the aqueous phase. All these substrates can be converted completely by hydrothermal reaction in the presence of catalyst, and the results were listed in Table I. As a control, rGO powder was directly used as the catalyst for fructose degradation, and 18% yield of lactic acid and 12.7% HMF (5-(hydroxymethyl)furfural) were detected, indicating that rGO itself is also a feeble catalyst for fructose conversion. The yield of lactic acid from fructose (Table I, entry 2) was higher than that of glucose (Table I, entry 3), and the product distribution for the conversion of glucose was almost the same as that of fructose, indicating that fructose may be a key intermediate for the conversion. Due to the β-1,4-glycosidic bonds in cellulose, it needs longer time to react, and the yield of lactic acid is 27.6% after 10 h reaction at 463 K (Table I, entry 4). When extra lactic acid was introduced to the system, the reaction time was significantly shortened and lactic acid yield 31.7% was attained in 4 h (Table I, entry 5), indicating that lactic acid played an autocatalytic function in this reaction which is also reported by Wang *et al.* [13]. However, the yield of lactic acid from cellulose is lower than that of Pb^{2+}

DOI:10.1063/1674-0068/28/cjcp1502026

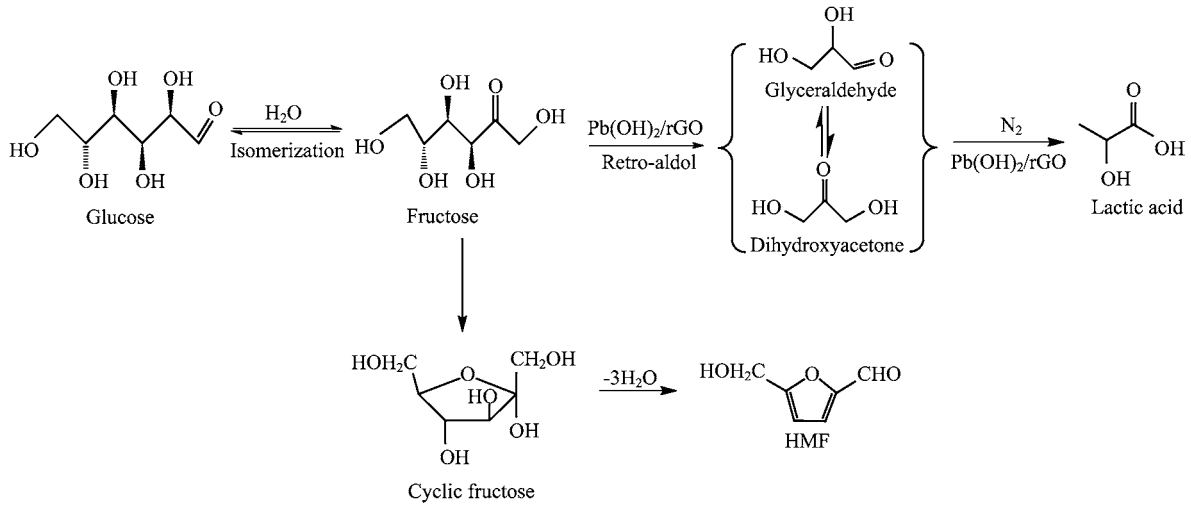

Scheme 1 Proposed mechanism for the conversion of glucose into lactic acid in water under N_2 atmospheres catalyzed by $Pb(OH)_2$/rGO.

ion catalysis, and the reason may be both cellulose and composite catalyst are in solid state which reduces the diffusion of lead inside the aggregates of cellulose, and the dissolving of cellulose in ionic liquid may promote the conversion, and it will be studied in near future.

Based on these results, a possible mechanism has been suggested for the conversion of glucose or fructose into lactic acid catalyzed by $Pb(OH)_2$/rGO (Scheme 1). At first, glucose needs an isomerization to fructose, then two C-3 intermediates glyceraldehyde and 1,3-dihydroxyacetone were formed by retro-aldol fragmentation of fructose, and lactic acid was formed at the end by catalysis of the trioses under N_2 atmosphere. In addition, it is also possible to form HMF via a side reaction.

Table II lists the results of the conversion of fructose over $Pb(OH)_2$/rGO (10%wt) catalyst for different reaction time, and the yield of lactic acid increased gradually from 0.5 h to 4 h. $Pb(OH)_2$/rGO catalyst with different mass loading of lead were also studied for their catalysis activity at 433 K, and the result is also listed in Table II. With in the low loading of 5wt%, only 31.6% of lactic acid was obtained while the yield increase to 58.7% when the mass loading of lead is 20wt%. Temperature is another key factor for the reaction, and as shown in Table II, the maximum yield of lactic acid was obtained when the reaction was carried out at 433 K.

Reusability is critical for prospective uses in industrial scale applications. Herein, we assessed the stability of the catalyst by catalyst recycle experiments (Table III). For the catalyst with a 20wt% Pb loading, the yield of lactic acid is 58.7% for the first run, and it was 52.8% for the second run, indicating that the catalyst is stable. During the third run, the yield of lactic acid is just 41.4%. ICP measurement has been used to measure the concentration of Pb^{2+} ion in the filtrate after three cycles, and about 16% of lead in the catalyst was leached. XPS, Raman, and FT-IR studies have also been carried out to measure the structure of the used catalyst, and as shown in Fig.3(b), Fig.5, and Fig.6. Clearly, the catalyst is relatively stable and can be used for three cycles. In this study, the yield of lactic

TABLE II Effect of reaction time t, Pb-contents c, and reaction temperature T on the yield of lactic acid (LA) in the conversion of fructose catalyzed by $Pb(OH)_2$/rGO.

t^a/h	LA/%	c^b/wt%	LA/%	T^c/K	LA/%
0.5	34.7	5	31.6	393	12.5
1	36.7	10	48.9	413	20.0
2	41.5	15	46.6	433	48.9
3	42.7	20	58.7	463	41.5
4	44.8			483	39.5

[a] Reaction condition: fructose of 65 mg, $Pb(OH)_2$/rGO (10wt%) of 25 mg, H_2O of 15 mL, N_2 of 2.5 MPa, 463 K.
[b] Reaction condition: fructose of 65 mg, $Pb(OH)_2$/rGO of 25 mg, H_2O of 15 mL, N_2 of 2.5 MPa, 463 K, 2 h.
[c] Reaction condition: fructose of 65 mg, $Pb(OH)_2$/rGO (10wt%) of 25 mg, H_2O of 15 mL, N_2 of 2.5 MPa, 2 h.

TABLE III Catalyst stability and recyclability of the catalyst.

Cycle	Lactic acid/%	
	10wt%	20wt%
1	48.9	58.7
2	44.1	52.8
3	38.2	41.4

Reaction condition: substrate of 65 mg, $Pb(OH)_2$/rGO of 25 mg, H_2O of 15 mL, N_2 of 2.5 MPa, 2 h.

DOI:10.1063/1674-0068/28/cjcp1502026

acid is lower than that reported by Wang *et al.*, where Pb^{2+} ion was used directly as a catalyst [13]. However, the amount of lead used here is much lower. For example, the molar ratio of glucose to $Pb(OH)_2$ here is 30:1 or 15:1 while the ratio was 3.64 in Wang's report, and clearly the fixation of $Pb(OH)_2$ nanoparticles onto the surface of rGO should reduce the amount of catalyst with an increasing efficiency.

IV. CONCLUSION

rGO nanosheets have been used as the support for $Pb(OH)_2$ nanoparticle, and the as-prepared catalyst was used to degrade biomass-based sugar to lactic acid, and various kinds of sugar from monosaccharide (fructose and glucose) and cellulose can be successfully dehydrated to lactic acid in aqueous solution or suspension, and the catalyst can be reused, and yields of lactic acid are 58.7%. The amount of $Pb(OH)_2$ used here is much lower than that of Pb^{2+} ion catalysis, and the fixation of $Pb(OH)_2$ nanoparticles on rGO nanosheets makes the catalyst easy to be handled and application in scale production of lactic acid from biomass.

V. ACKNOWLEDGMENTS

This work was supported by the National Basic Research Program of China (No.2011CB921403), the National Natural Science Foundation of China (No.51073147), and the Natural Science Foundation of Anhui Province (No.1408085MKL03).

[1] P. Maki-Arvela, I. L. Simakova, T. Salmi, and D. Y. Murzin, Chem. Rev. **114**, 1909 (2014).
[2] M. A. Abdel-Rahman, Y. Tashiro, and K. Sonomoto, Biotechnol. Adv. **31**, 877 (2013).
[3] C. Gao, C. Q. Ma, and P. Xu, Biotechnol. Adv. **29**, 930 (2011).
[4] M. Dusselier, P. Van Wouwe, A. Dewaele, E. Makshina, and B. F. Sels, Energy Environ. Sci. **6**, 1415 (2013).
[5] M. Moller, P. Nilges, F. Harnisch, and U. Schroder, ChemSusChem **4**, 566 (2011).
[6] C. Sánchez, I. Egüés, A. García, R. Llano-Ponte, and J. Labidi, Chem. Eng. J. **181/182**, 655 (2012).
[7] F. Jin and H. Enomoto, Energy Environ. Sci. **4**, 382 (2011).
[8] E. Taarning, C. M. Osmundsen, X. B. Yang, B. Voss, S. I. Andersen, and C. H. Christensen, Energy Environ. Sci. **4**, 793 (2011).
[9] X. Jin, D. Roy, P. S. Thapa, B. Subramaniam, and R. V. Chaudhari, Acs Sus. Chem. Eng. **1**, 1453 (2013).
[10] H. Wang, Y. Wang, Y. Chen, Q. Jin, and J. Ji, Polym. Chem. **5**, 854 (2014).
[11] F. F. Wang, C. L. Liu, and W. S. Dong, Green Chem. **15**, 2091 (2013).
[12] X. Jin, L. N. Dang, J. Lohrman, B. Subramaniam, S. Q. Ren, and R. V. Chaudhari, Acs Nano **7**, 1309, (2013).
[13] Y. Wang, W. Deng, B. Wang, Q. Zhang, X. Wan, Z. Tang, Y. Wang, C. Zhu, Z. Cao, G. Wang, and H. Wan, Nat. Commun. **4**, 2141 (2013).
[14] B. F. Machado and P. Serp, Cat. Sci. Technol. **2**, 54 (2012).
[15] J. Pyun, Angew. Chem. Int. Ed. **50**, 46 (2011) .
[16] X. Z. Wang, W. F. Chen, and L. F. Yan, Mater. Chem. Phys. **148**, 103 (2014).
[17] C. Z. Zhu and S. J. Dong, Nanoscale **5**, 1753 (2013).
[18] Y. Yao, X. Chen, J. Zhu, B. Zeng, Z. Wu, and X. Li, Nanoscale Res. Lett. **7**, 363 (2012).
[19] C. Hu, G. Zheng, F. Zhao, H. Shao, Z. Zhang, N. Chen, L. Jiang, and L. Qu, Energy Environ. Sci. **7**, 3699 (2014).
[20] W. F. Chen and L. F. Yan, Nanoscale **2**, 559 (2010).
[21] E. Culea, L. Pop, M. Bosca, T. Rusu, P. Pascuta, and S. Rada, J. Phys.: Conf. Ser. **182**, 012061 (2009).

DOI:10.1063/1674-0068/28/cjcp1502026